Author(s): Tuomisto, Filip & Paskova, T. & Kröger, R. & Figge, S. & Hommel, D. & Monemar, B. & Kersting, R.

Title: Defect distribution in a-plane GaN on Al2O3

Year: 2007

Version: Final published version

Please cite the original version:

Tuomisto, Filip & Paskova, T. & Kröger, R. & Figge, S. & Hommel, D. & Monemar, B. & Kersting, R. 2007. Defect distribution in a-plane GaN on Al2O3. Applied Physics Letters. Volume 90, Issue 12. 121915/1-3. ISSN 0003-6951 (printed). DOI: 10.1063/1.2715128

Defect distribution in a -plane GaN on Al 2 O 3

F. Tuomisto, T. Paskova, R. Kröger, S. Figge, D. Hommel, B. Monemar, and R. Kersting

Citation: Applied Physics Letters **90**, 121915 (2007); doi: 10.1063/1.2715128
View online: http://dx.doi.org/10.1063/1.2715128
View Table of Contents: http://scitation.aip.org/content/aip/journal/apl/90/12?ver=pdfcov
Published by the AIP Publishing

Defect distribution in *a*-plane GaN on Al_2O_3

F. Tuomisto[a)]
Laboratory of Physics, Helsinki University of Technology, FI-02015 TKK, Finland

T. Paskova, R. Kröger, S. Figge, and D. Hommel
Institute of Solid State Physics, University of Bremen, D-28359 Bremen, Germany

B. Monemar
Department of Physics and Measurement Technology, Linköping University, S-58183 Linköping, Sweden

R. Kersting
Tascon GmbH, D-48148 Münster, Germany

(Received 21 December 2006; accepted 15 February 2007; published online 22 March 2007)

The authors studied the structural and point defect distributions of hydride vapor phase epitaxial GaN film grown in the [11−20] *a* direction on (1−102) *r*-plane sapphire with metal-organic vapor phase deposited *a*-GaN template using transmission electron microscopy, secondary ion mass spectrometry, and positron annihilation spectroscopy. Grown-in extended and point defects show constant behavior as a function of thickness, contrary to the strong nonuniform defect distribution observed in GaN grown along the [0001] direction. The observed differences are explained by orientation-dependent and kinetics related defect incorporation. © *2007 American Institute of Physics*. [DOI: 10.1063/1.2715128]

Recently, there has been an emerging interest in the growth of nonpolar III-nitrides for optoelectronic device structures free of polarization-induced electric fields. Combining this with the possibility of growing thick GaN films by hydride vapor phase epitaxy (HVPE) is expected to lead to nonpolar GaN layers with low dislocation density. A large effort has been devoted to structural characterization of this material and to the improvement of the crystal quality.[1–5] However, the point defect distribution in nonpolar GaN is relatively poorly understood.

The growth polarity has a dramatic effect on the ingrown point defects in HVPE-grown *c*-plane GaN. The incorporation of impurities and formation of vacancy defects are significantly enhanced in growth in the N polar (as opposed to Ga polar) direction.[6] These defects define the electrical, optical, and structural qualities of the material. In addition, in heteroepitaxial *c*-plane GaN grown on *c*-plane sapphire the distribution of impurities and native defects is nonuniform and their concentration decreases with the distance from the GaN/sapphire interface.[7–10]

In this work we use transmission electron microscopy (TEM), secondary ion mass spectrometry (SIMS), and positron annihilation spectroscopy (PAS) to study the distribution of both extended and point defects in *a*-plane HVPE GaN grown on an *a*-plane GaN template grown by metal-organic chemical vapor deposition (MOCVD) on *r*-plane sapphire. We compare the results to those obtained earlier in *c*-plane HVPE GaN.[6] We propose an orientation-dependent defect incorporation model based on kinetics considerations to account for the differences in the defect distributions.

We studied a series of four *a*-plane GaN samples, one MOCVD *a*-GaN layer with a thickness of 1.2 μm and three HVPE *a*-GaN films with thicknesses of about 5, 18, and 25 μm, grown on *r*-plane sapphire by employing the same thin *a*-plane MOCVD GaN template. The HVPE growth was carried out at Linköping University in a conventional horizontal HVPE reactor at 1080 °C (Ref. 5) and V/III ratio of 7. The GaN templates, including SiN micromask aiming at threading dislocation reduction, were grown at Bremen University in a Thomas Swan vertical reactor at 1050 °C and V/III ratio in the range of 2400–3000.

A three-dimensional impurity analysis was performed by time-of-flight secondary ion mass spectrometry using an ION TOF TOF.SIMS 5 instrument. For a quantitative analysis of the oxygen concentration in the GaN film Cs^+ sputtering and Bi^+ analyzing beams were used. Figure 1 shows an oxygen SIMS image of the cross section of one representative sample with total GaN thickness of about 18 μm. The O concentration remains almost constant in each of the sublayers with a very strong contrast between them, it is $\sim 1 \times 10^{17}$ and $\sim 3 \times 10^{18}$ cm^{-3} in the MOCVD GaN and HVPE GaN, respectively. The higher O concentration in the HVPE material as compared to the MOCVD material is in agreement with previously observed trends in the residual impurity concentrations in *c*-plane GaN.[11,12] The increase of the O concentration at the MOCVD-HVPE GaN interface could be tentatively attributed to nonfully optimized surface pretreatment before the HVPE overgrowth. The almost constant behavior of the O concentration along the thickness, which is in strong contrast with the strong nonuniform distribution of the O content, ranging over a few orders of magnitude, observed in GaN grown in the *c* direction.[7,11]

For the microstructural analysis of extended defects such as basal plane stacking faults (BSFs), a cross-section TEM specimen was prepared in the [1−100] orientation by mechanical polishing followed by Ga ion milling in a NOVA Nanolab (FEI) dual beam focused ion beam system operated at 30 kV. Three cross-sectional TEM images taken at the HVPE GaN (spot 1), HVPE-MOCVD GaN interface (spot 2), and MOCVD GaN (spot 3) areas are shown in Figs. 1(b)–1(d), respectively. Since the imaging was performed in the [1−100] zone axis and the sample was slightly tilted

a)Electronic mail: filip.tuomisto@tkk.fi

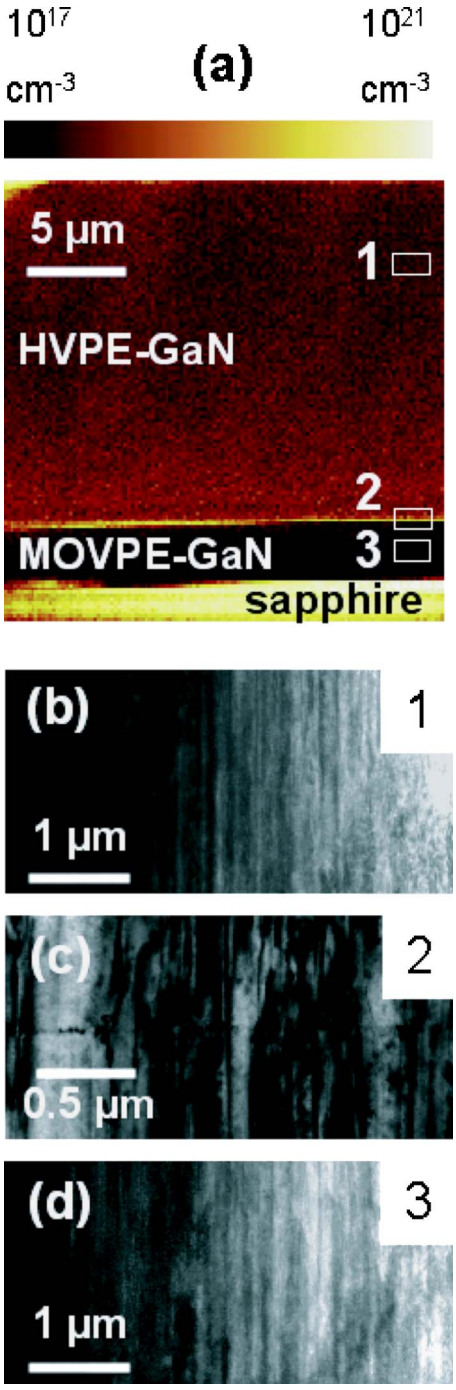

FIG. 1. (Color online) (a) Cross-sectional SIMS image showing the oxygen distribution in the sapphire/MOCVD-grown *a*-GaN/HVPE-grown *a*-GaN. The quantification is only valid for the GaN film and the dimensions of the image are 22 and 90 μm in the *x* and *y* directions, respectively. [(b)–(d)] Cross-sectional TEM images taken in spots 1–3, respectively, as indicated in (a). The zone axis for the TEM imaging is [0001], showing nearly constant BSF distribution along the thickness of the structure.

towards the [0001] direction, the BSFs are clearly visualized. Their density remains constant and comparable along the two MOCVD and HVPE layers with no noticeable change at the interface [Fig. 1(c)]. The density of the BSFs was determined to be about 5×10^5 cm^{-2}. As the BSFs are bonded by Frank-Shockley partial dislocations,[13] the dislocation density was estimated to be in the order of 10^{10} cm^{-2}, maintaining this value throughout the whole thickness.

We studied the distribution of the vacancy defects along the growth *a* axis with a variable energy (E=0–38 keV)

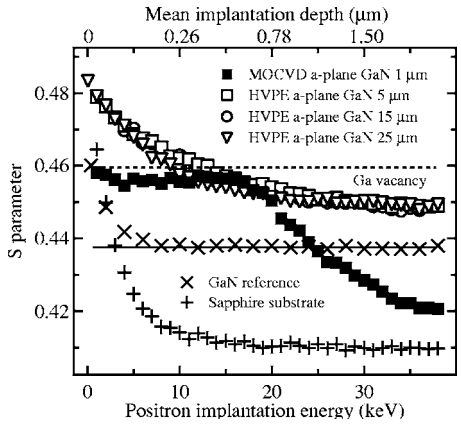

FIG. 2. *S* parameter in the *a*-plane GaN layers as a function of positron implantation energy. The solid and dashed lines show the *S* parameter in the GaN lattice and at a Ga vacancy, respectively. Also the *S* parameters measured in the GaN reference and in the sapphire substrate are shown.

positron beam. The trapping of positrons at vacancy defects can be observed as the narrowing of the Doppler-broadened 511 keV annihilation peak. The measured spectra were characterized by the conventional line shape parameters *S* and *W*.[14,15] Figure 2 shows the *S* parameter measured in the GaN samples as a function of positron implantation energy (depth scan). The *S* parameter measured in the *a*-plane GaN layers is above the value in the defect-free GaN lattice, indicating that positrons are trapped at vacancy defects. Interestingly, the *S* parameters measured in the 5–25 μm thick HVPE samples are similar and saturate at high positron implantation energies to a value slightly lower than that in the MOCVD GaN template (at the region at 5–15 keV). The *S* parameter measured in the HVPE layers decreases with the distance from the sample surface clearly slower than in the GaN reference, indicating that the near-surface region (first few hundred nanometers) contains vacancy defects with a concentration significantly higher than that in the bulk of the layer.

The vacancy defects observed in the *a*-plane GaN layers have been already identified using both the *S* and *W* parameters as V_{Ga}-O_N pairs.[15] This is in line with previous studies[6,9,10,16] that have shown that the V_{Ga}-O_N pair is the dominant in-grown vacancy defect observed with positrons in HVPE GaN. The concentrations of the observed V_{Ga}-O_N pairs in the *a*-plane GaN layers can be estimated from the (S,W) parameters [14] using a typical positron trapping coefficient of $\mu_V=3\times10^{15}$ s^{-1} for the Ga vacancy. The estimated values are $[V_{Ga}]=1\times10^{18}$ cm^{-3} in the MOCVD GaN template and $[V_{Ga}]=2\times10^{17}$ cm^{-3} in the 5–25 μm thick HVPE layers. The behavior of the V_{Ga} concentration as a function of distance from the GaN/sapphire interface in these *a*-plane HVPE GaN layers is strikingly different from that in the *c*-plane HVPE GaN (see Fig. 3).

In the *c*-plane HVPE GaN, the V_{Ga} concentration decreases by more than two orders of magnitude when the distance from the interface increases from 1 to 30 μm,[9] and there is a strong correlation with the distributions of the O impurities and dislocations. Our results in *a*-plane HVPE GaN show that the distributions of the BSFs, O impurities, and V_{Ga} are all constant as a function of the distance (from 5 to 25 μm) from the interface. Therefore, point defect densities follow the density of extended defects for both *a*-plane and *c*-plane HVPE GaN. Interestingly, there are significant

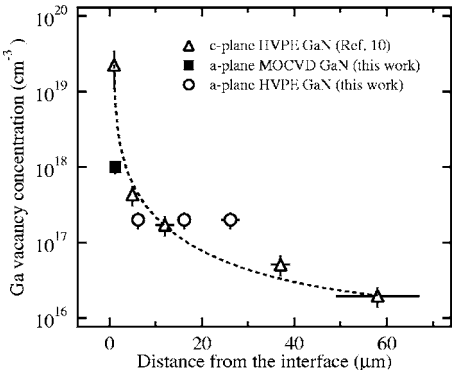

FIG. 3. Estimated Ga vacancy concentrations as a function of the distance from the sapphire interface. The values for *c*-plane HVPE GaN are taken from Ref. 9.

differences between the *a*-plane HVPE and MOCVD layers: the O concentration is almost one order of magnitude lower in the *a*-plane MOCVD GaN layer than in HVPE GaN, while the concentrations of the stacking faults are similar and the concentrations of the Ga vacancies are higher. Especially the behavior of the O impurity and Ga vacancy concentrations is unexpected, as they have been shown to correlate individually both in *c*-plane MOCVD and HVPE GaN.[16,17]

The spatial correlation of the densities of O impurities and dislocations in *c*-plane HVPE GaN grown on sapphire has been attributed to the dislocation-mediated diffusion of oxygen from the substrate.[7] On the other hand, a high O impurity (about 10^{19} cm^{-3}) concentration has been found to also exist in homoepitaxial N-polar HVPE GaN, where the dislocation density is already several orders of magnitude lower at the interface than in heteroepitaxial GaN. This has been attributed to the enhanced incorporation of impurities on some growth surfaces relative to the others.[6,18] As the growth of N-polar GaN proceeds with a strong contribution of nonpolar lateral growth modes, the efficient incorporation of impurities from the growth environment is a likely cause for the high O impurity concentration in *a*-plane HVPE GaN as well. Hence our results suggest that the nonpolar growth mode determines the O impurity incorporation in heteroepitaxial *a*-plane GaN, while the impact of the BSF and partial dislocations connected with them is negligible.

The reverse ratio of the O impurity and Ga vacancy concentrations in the *a*-plane HVPE and MOCVD GaN layers is more complicated. We propose that the differences in the point defect distributions in these materials arise from the different growth environments and are additionally affected by the interplay of the O impurities and dislocations. The MOCVD growth is clearly more N rich than the HVPE growth, and hence from kinetics point of view the incorporation of the O_N should be more efficient in the latter in an otherwise defect-free crystal. With the same argument, the V_{Ga} formation should be more efficient in MOCVD-grown GaN. (i) In *c*-plane material intentionally doped with O to similar concentrations, the Ga vacancy concentration in MOCVD GaN is indeed at least one order of magnitude higher than in HVPE GaN.[15,16] However, the differences in the incorporation of unintentional O from the growth environment are much less evident. This on the other hand can be explained by high density of dislocations whose presence dominates the O incorporation as the O concentration has been shown to be clearly lower in dislocation-free homoepitaxial HVPE GaN.[6] (ii) In *a*-plane GaN, where the O incorporation is independent of the distance from the substrate and hence seems to be dominated by the higher reactivity of the nonpolar growth surface compared to the *c*-plane material, the behavior of both the O impurities and Ga vacancies follows the above-presented kinetic trends rather well.

In summary, we have investigated the distributions of extended and point defects in *a*-plane heteroepitaxial GaN using SIMS, TEM, and PAS. We show that unlike in *c*-oriented GaN, the defect (O impurity, Ga vacancy, and BSF) distributions do not vary significantly in *a*-plane HVPE GaN as a function of distance from the GaN/sapphire interface. We propose an orientation-dependent defect incorporation model based on kinetics considerations to account for the anticorrelations of the point defect concentrations in the *a*-plane MOCVD GaN and *a*-plane HVPE GaN.

[1]M. D. Craven, F. Wu, S. H. Lim, J. S. Speck, and S. P. Denbaars, Appl. Phys. Lett. **81**, 1201 (2002).
[2]B. A. Haskell, F. Wu, M. D. Craven, S. Matsuda, P. T. Fini, T. Fujii, K. Fujito, S. P. Denbaars, J. S. Speck, and S. Nakamura, Appl. Phys. Lett. **83**, 644 (2003).
[3]B. A. Haskell, T. J. Baker, M. B. McLaurin, F. Wu, P. T. Fini, S. P. Denbaars, J. S. Speck, and S. Nakamura, Appl. Phys. Lett. **86**, 111917 (2005).
[4]B. A. Haskell, A. Chakraborty, F. Wu, H. Sasano, P. T. Fini, S. P. Denbaars, J. S. Speck, and S. Nakamura, J. Electron. Mater. **34**, 357 (2005).
[5]T. Paskova, V. Darakchieva, P. P. Paskov, J. Birch, E. Valcheva, P. O. A. Persson, B. Arnaudov, S. Tungasmita, and B. Monemar, J. Cryst. Growth **281**, 55 (2005).
[6]F. Tuomisto, K. Saarinen, B. Lucznik, I. Grzegory, H. Teisseyre, T. Suski, S. Porowski, P. Hageman, and J. Likonen, Appl. Phys. Lett. **86**, 031915 (2005).
[7]D. C. Look, C. E. Stutz, R. J. Molnar, K. Saarinen, and Z. Liliental-Weber, Solid State Commun. **117**, 571 (2001).
[8]X. L. Sun, S. H. Goss, L. J. Brillson, D. C. Look, and R. J. Molnar, J. Appl. Phys. **91**, 6729 (2002).
[9]J. Oila, J. Kivioja, V. Ranki, K. Saarinen, D. C. Look, R. J. Molnar, S. S. Park, S. K. Lee, and J. Y. Han, Appl. Phys. Lett. **82**, 3433 (2003).
[10]F. Tuomisto, K. Saarinen, T. Paskova, B. Monemar, M. Bockowski, and T. Suski, J. Appl. Phys. **99**, 066105 (2006).
[11]T. Paskova, P. P. Paskov, V. Darakchieva, E. M. Goldys, U. Södervall, E. Valcheva, B. Arnaudov, and B. Monemar, Phys. Status Solidi C **0**, 209 (2002).
[12]A. E. Wickenden, D. D. Koleske, R. L. Henry, M. E. Twigg, and M. Fatemi, J. Cryst. Growth **260**, 54 (2004).
[13]R. Kröger, T. Paskova, B. Monemar, S. Figge, D. Hommel, and A. Rosenauer, Proceedings of the International Workshop on Nitride Semiconductors (IWN2006), 22–27 October 2006, Kyoto, Japan (unpublished).
[14]K. Saarinen, P. Hautojärvi, and C. Corbel, in *Identification of Defects in Semiconductors*, edited by M. Stavola (Academic, New York, 1998), Vol. 51A, p. 209.
[15]F. Tuomisto, T. Paskova, S. Figge, D. Hommel, and B. Monemar, J. Cryst. Growth **300**, 251 (2007).
[16]S. Hautakangas, V. Ranki, I. Makkonen, M. J. Puska, K. Saarinen, X. Xu, and D. C. Look, Phys. Rev. B **73**, 193301 (2006).
[17]J. Oila, V. Ranki, J. Kivioja, K. Saarinen, P. Hautojärvi, J. Likonen, J. M. Baranowski, K. Pakula, T. Suski, M. Leszczynski, and I. Grzegory, Phys. Rev. B **63**, 045205 (2001).
[18]E. Frayssinet, W. Knap, S. Krukowski, P. Perlin, P. Wisniewski, T. Suski, I. Grzegory, and S. Porowski, J. Cryst. Growth **230**, 442 (2001).